

Clinical Pearls for Success in Femto-LASIK Refractive Surgery

We have 3 months of experience using the Femto LDV in combination with the Amaris Total Tech Laser.

BY MARIA CLARA ARBELAEZ, MD; AND SAMUEL ARBA MOSQUERA, MS

Laser refractive surgery has evolved full circle. Surface ablations (PRK) swiftly evolved into intrastromal corrections (LASIK) due to faster visual recovery and minimized postoperative discomfort. However, as the adoption of LASIK grew, there was more concern about post-LASIK keratectasia. Therefore, we have witnessed a renewed interest in advanced surface ablation over the past few years to avoid LASIK complications, primarily corneal ectasia and flap- and interface-related problems.

In parallel, laser refractive surgery has evolved from simple myopic ablations¹ to sophisticated, topography-guided² and wavefront-driven³ platforms, either using wavefront measurements of the whole eye⁴ (eg, obtained by Hartmann-Shack wavefront sensors) or using corneal topography-derived wavefront analyses^{5,6} to design customized ablation patterns.

Corneal ablations induce aberrations; one of the most significant side effects in myopic LASIK is the induction of spherical aberration,⁷ which causes halos and reduces contrast sensitivity.⁸ To combat these aberrations, special ablation patterns are needed to preserve the preoperative level of higher-order aberrations (HOAs).⁹⁻¹¹ The focus has now moved from primary refractive outcomes to effects of the ablation on postoperative HOAs. Achieving accurate clinical outcomes and reducing the likelihood of a retreatment procedure are major goals of any refractive procedure.

The introduction of ocular wavefront measurements and customized correction has brought another dimension to the debate between surface ablation and intrastromal correction. Newer ablation profiles have been introduced, such as the aspheric profile, which aims to maintain the normal prolate shape of the cornea, and the aberration-free profile, which aims to maintain the normal preexisting aberrations



Figure 1. The Femto LDV and Amaris systems integrate to form the Z-LASIK workstation on which LASIK can be performed as a seamless procedure.

of the eye. Furthermore, surface ablation may be better suited for wavefront-guided ablation technology because it avoids flap- and interface-induced aberrations;^{12,13} however, because of the introduction of thin and ultra-thin planar flaps created by the femtosecond laser and newer microkeratomes, such as the Carriazo-Pendular microkeratome (Schwind eye-tech-solutions; Kleinostheim, Germany) this aspect of the debate will require further research.

PEARLS FOR FEMTO-LASIK SUCCESS

In this article, we discuss several pearls for successful femtosecond LASIK (femto-LASIK or Z-LASIK) treatments, such as how to avoid ablation of the flap edges, hinge, and inner face of the disc. It is difficult to talk about pearls when, as in this case, results were excellent from the first treatment on the first day. There were no complications, adverse events, or unsatisfactory outcomes. However, we can relay several pointers regarding

TAKE-HOME MESSAGE

- Femto-LASIK maximizes outcomes by minimizing tissue removal.
- Plan treatments with large optical zones.
- The flap should have a large diameter—specifically 9, 9.5, or 10 mm.
- The Aberration-Free aberration-neutral profile leaves the visual print of the patient as it was preoperatively with the best spectacle correction.

what one should focus on when learning femto-LASIK surgery.

Residual corneal thickness. It is important to make sure that the patient's predicted postoperative residual corneal thickness remains thicker than three-quarters of his preoperative pachymetry. This will ensure that corneal biomechanical reactions are not excessively stressed.¹⁴ In myopic patients, the immediate postoperative residual stromal thickness, prior to reflecting back the flap, must remain thicker than three-fifths of the preoperative pachymetry. Again, this ensures that there is no excessive stress on corneal biomechanical reactions.¹⁵ An online pachymeter, preferably noncontact, is mandatory.¹⁶ In hyperopic patients, the predicted residual corneal thickness must remain thicker in the periphery than at the center. By doing this, the natural corneal pachymetry peripheral ratio will not be disrupted.¹⁷

Ablation profiles. The use of aspheric¹⁸ (Aberration-Free profile, available with the Amaris Total Tech Laser; Schwind eye-tech-solutions) ablation volumes compensates for parameters including corneal biomechanical effects, flap cut, and intraocular pressure. The Aberration-Free profile is aspheric-based¹⁸ and includes a multidynamic aspheric transition zone, aberration and focus shift compensation due to tissue removal, pseudo-matrix-based spot positioning, enhanced compensation for the loss of efficiency,¹⁸ and intelligent thermal effect control. All of these characteristics are based on theoretical equations validated with ablation models and clinical evaluations.

Make sure that whatever system you use considers keratometry readings to compensate for the loss of ablation efficiency effects.¹⁹ Additionally, pay attention to the different laser-tissue interaction properties for corneal surface and stromal tissues²⁰ (or make sure your system does it for you).

Do not waste tissue. Rather, maximize outcomes by minimizing tissue removal. As a general rule, use aspheric treatments if the patient has no symptomatic aberrations and his BCVA is 20/20 or better.²¹ Reserve customized

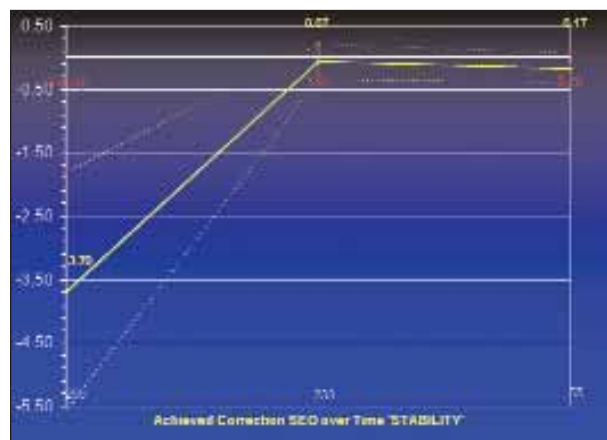


Figure 2. Stability plot: Progression of refraction over time.

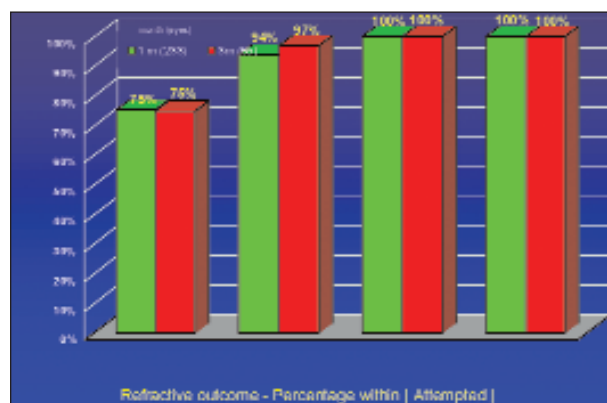


Figure 3. Achieved refractive outcome at 1 and 3 months.

ablation treatments for special needs, such as:

- Ocular wavefront in patients with symptomatic aberrations and an initial BCVA worse than 20/20;
- Corneal wavefront in patients with symptomatic aberrations,²² an initial BCVA worse than 20/20, and a small pupil; and
- Corneal wavefront in patients who needed retreatment and have a BCVA worse than 20/20.

Plan your treatments in large optical zones. I use smart blending zones, which avoid edge effects, especially in coma and spherical aberration.²³ Center your treatments in an optimized way:

- For aspheric treatments, the center should refer to the corneal vertex.²⁴ Modification of the corneal sphere is established with the Aberration-Free ablation profile.
- For customized wavefront treatments (based on diagnosed aberrations), use the aberration maps as a description/reference system for the pupil center, where the center refers to the entrance pupil (as measured in diagnosis).

Flap creation. Create large flap discs (greater than 9 mm), using a 9-mm marker to ensure perfect centration and

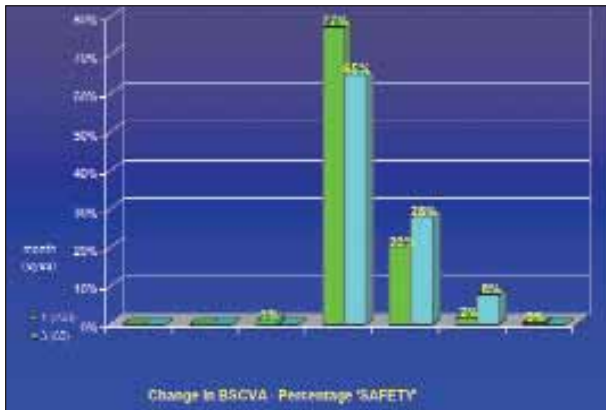


Figure 4. Safety plot: change in BCVA at 1 and 3 months.

objectively measure the amount of ablation to achieve perfect flaps in terms of centration and size. Use a nasal hinge for optimized outcomes²⁵ or a superior hinge for maximum safety. Additionally, thin flaps²⁶ minimize cutting of corneal nerves. Cross-check your actual flap thickness by performing intraoperative pachymetry.²⁷ We prefer to use a noncontact, online pachymeter.

RETROSPECTIVE ANALYSIS

We retrospectively analyzed results from the first 250 eyes we treated with the combined use of the Amaris Aberration-Free aspheric ablation profiles and the Ziemer Femto LDV (Ziemer Group AG, Port, Switzerland). One-month follow-up was available for 233 eyes; 3-month follow-up for 65 eyes.

All ablations were noncustomized, based on aberration neutral profiles, and calculated using the ORK-CAM software module (Optimized Refractive Keratectomy-Custom Ablation Manager; Schwind eye-tech-solutions). Aspheric aberration-neutral profiles, such as Schwind's Aberration-Free, add aspheric characteristics to balance the induced spherical aberration.^{28,29}

METHOD

A 6.5-mm, central, fully corrected ablation zone was used in all eyes. The laser automatically provided a variable transition size (6.7–8.6 mm), which was related to the planned refractive correction. The ablation was performed using the Amaris excimer laser. The laser's randomized flying-spot ablation pattern and control of local repetition rates, to minimize the treatment's thermal load,³⁰ keep the ablated surface smooth when the aspheric aberration-neutral profile is used. Theoretically, these optimizations diminish induction of wavefront aberrations after myopic LASIK.

All flaps were created using the Femto LDV femtosecond laser; the nominal flap thickness was 110 μ m, and

CRSTodayEurope.com

CRSTodayEurope.com

CRSTodayEurope.com

CRSTodayEurope.com

CRSTodayEurope.com

CRSTodayEurope.com

CRSTodayEurope.com

CRSTodayEurope.com

CRSTodayEurope.com

CRSTodayEurope.com

CRSTodayEurope.com

CRSTodayEurope.com

visit www.crstodayeurope.com for the current issue and complete archives

CRSTodayEurope.com

CRSTodayEurope.com

CRSTodayEurope.com

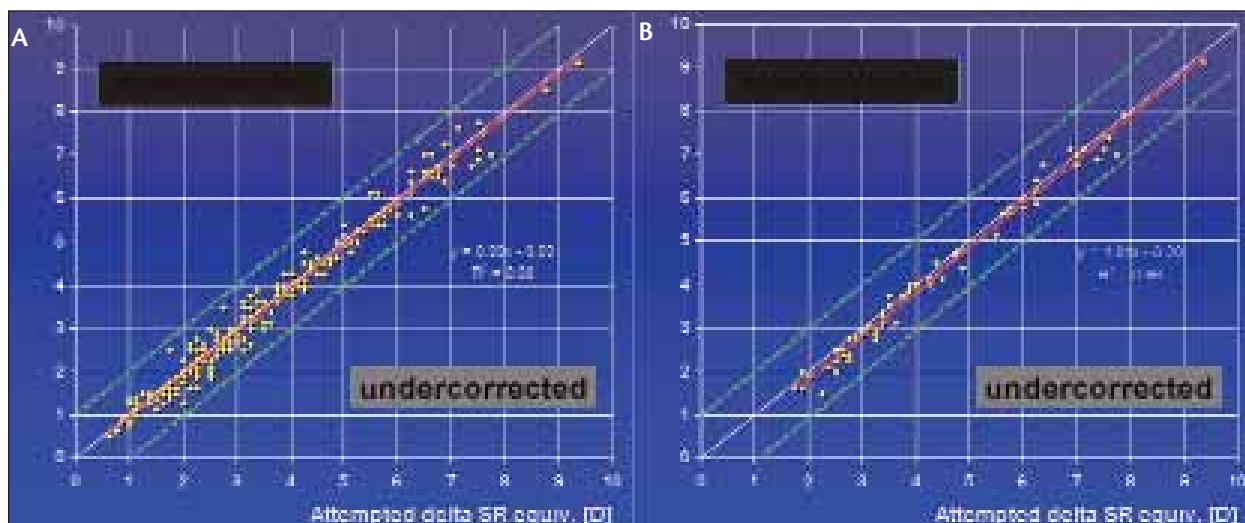


Figure 5. Achieved versus attempted corrections at (A) 1- and (B) 3-month follow-up.

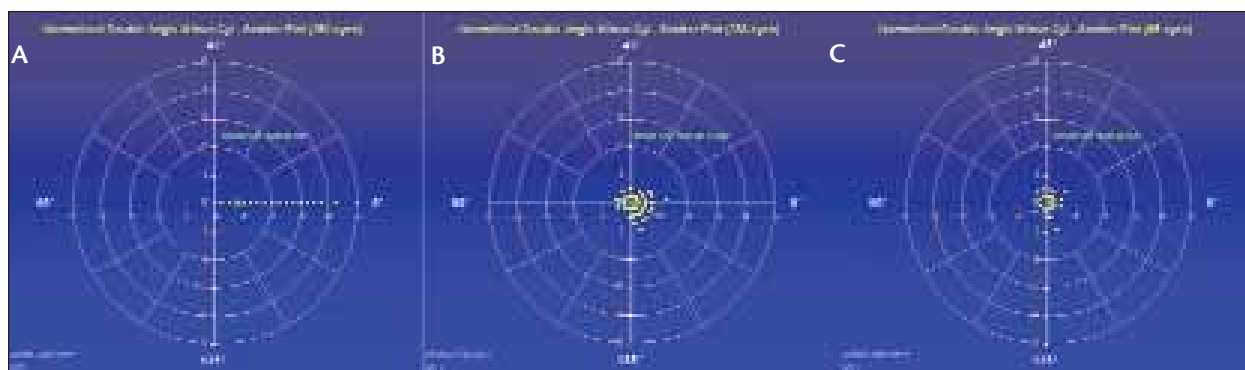


Figure 6. Refractive astigmatism (A) preoperatively and at (B) 1- and (C) 3-month follow-up.

the nominal flap diameter was 9 mm or 9.5 mm. Optical errors centered on the line of sight, and the standardized diameter was 6 mm for corneal wavefront.

RESULTS

Neither adverse events nor complications were observed intra- or postoperatively. No eye needed or demanded a retreatment.

Flap predictability. The mean achieved flap thickness was $104 \pm 7 \mu\text{m}$ (range, 93–126 μm). The mean achieved flap diameter was $9.2 \pm 0.2 \mu\text{m}$ (range, 8.5–9.5 mm) when the 9-mm diameter was used, and $9.7 \pm 0.3 \mu\text{m}$ (range, 9–10 mm) when the 9.5-mm diameter was used.

Refractive outcome. At 1 month postoperatively, the mean residual defocus refraction was $-0.07 \pm 0.28 \text{ D}$ (range, -0.75 to 1.00 D ; $P < .0001$); mean residual astigmatism magnitude was $0.23 \pm 0.23 \text{ D}$ (range, 0.00–1.25 D; $P < .0001$; Table 1). Seventy-five percent of eyes were within 0.25 D of attempted correction, and 100% percent of

eyes were within 1.00 D of attempted correction.

At 3 months postoperatively, the mean residual defocus refraction was $-0.17 \pm 0.22 \text{ D}$ (range, -0.75 to 0.38 D ; $P < .0001$; Figure 2); the mean residual astigmatism magnitude was $0.21 \pm 0.21 \text{ D}$ (range, 0.00–1.00 D; $P < .0001$). Seventy-five percent of eyes were within 0.25 D of attempted correction, and 100% percent eyes were within 1.00 D (Figure 3).

Safety. Twenty percent of eyes gained one line and 3% gained two or more lines of BCVA at 1 month ($P < .01$), whereas 28% gained one line and 8% gained two or more lines at 3 months ($P < .005$; Figure 4).

Predictability. The achieved refractive change significantly correlated with the intended correction ($r^2 = .99$; $P < .0001$). The regression slope (1.0) was similar to the ideal correction (Figure 5), and the achieved changes in cardinal and oblique astigmatisms significantly correlated with the intended corrections (Figure 6).

Changes in corneal wavefront aberration. No single

aberration Zernike term (Table 1) changed significantly after treatment. For all of them, the variation was well below clinical relevance.

DISCUSSION

This consecutive series includes the surgeons' learning curve with femto-LASIK, plus the use of two new devices (Femto LDV and the Amaris Total Tech Laser).

The Aberration-Free ablation profile has the advantage of being neutral in regard to HOAs, leaving the visual print of the patient as it was preoperatively with the best spectacle correction. In our group of patients, we observed a minor increase in corneal aberrations at 6 mm; however, none of our patients required retreatment, and spherical and astigmatic results were stable at 3 months. Longer follow-ups and a larger number of eyes are recommended to confirm stability.

At 1 and 3 months, no single eye lost any lines of BCVA, and seven and five eyes gained two or more lines, respectively ($P < .005$). The average residual defocus and cylinder were -0.20 D and 0.20 D, respectively, with more than 94% of patients within 0.50 D of the target correction. No flap complications occurred.

As shown by our data, Z-LASIK with the Femto LDV and Amaris platforms is safe and effective, and outcomes in our study were better for this population relative to previous laser platforms. These improvements may be related to the ability of the high-speed Amaris system to reduce variability from stromal hydration effects^{31,32} and the low pulse energy of the Femto LDV, which also produces tiny cavitation bubbles during flap creation. Long-term follow-up will determine whether these accurate results also show improved stability compared with previous experiences.

The most important determination for refractive results is the performance of the ablative laser system and the treatment profiles; however, flap complications can impair the performance of the excimer laser. For this reason, the combination of the Femto LDV and the Amaris is particularly interesting. The femtosecond laser may customize the hinge position of the flap in any direction—superior, nasal, or temporal—and minimize the size of the hinge (typically, 0.4 mm).

It is important to mention the versatility of the two machines together: Both are compact; there is no waiting time between flap and ablation because the same patient bed is used; and both are stable, reliable, and easy to maintain. Additionally, patients reported excellent visual performance after Z-LASIK. This finding may be attributed to the thin, planar, and reproducible flaps created with the Femto LDV. All flaps were free of

TABLE 1. COMPARISON OF REFRACTION AND INDUCED ABERRATIONS AFTER REFRACTIVE SURGERY

	Preoperative (mean \pm SD)	3-month postoperative (mean \pm SD)
Spherical Equivalent (D)	-3.71 \pm 1.90 D	-0.17 \pm 0.22 D
Cylinder (D)	0.80 \pm 0.84 D	0.21 \pm 0.21 D
Predictability within \pm 0.50 D (%)	NA	93%
Predictability within \pm 1.00 D (%)	NA	100%
Spherical Aberration C[4,0] at 6 mm (μ m)	0.20 \pm 0.13	0.17 \pm 0.08
Coma C[3, -1] at 6 mm (μ m)	0.01 \pm 0.19	0.08 \pm 0.13
Coma C[3, +1] at 6 mm (μ m)	-0.06 \pm 0.10	-0.02 \pm 0.15
Trefoil C[3, -3] at 6 mm (μ m)	-0.01 \pm 0.13	-0.08 \pm 0.15
Trefoil C[3, +3] at 6 mm (μ m)	-0.02 \pm 0.12	0.00 \pm 0.11
Higher-order aberration at 6 mm (μ m RMS)	0.38 \pm 0.11	0.30 \pm 0.08

edema, opacification, and inflammatory reactions—most likely result of the laser's low pulse energy.

Despite large defocus and astigmatism magnitudes, our study showed that HOAs are either minimally increased or unchanged after surgery with the LDV and Amaris systems (Table 1). Postoperative complaints of HOAs, such as coma and spherical aberration, were the result of decentration and edge effects from the strong local curvature change from the optical to transition zone and from the transition zone to untreated cornea.

It is necessary to emphasize the use of large optical zones, covering the scotopic pupil size plus some tolerance for possible decentration, and well-defined smooth transition zones. For optimal outcomes with minimal induced aberrations, the flap should have a large diameter (9, 9.5, or 10 mm).

Although our small series of treated eyes does not allow definitive conclusions or evidence-based statements, our preliminary results are promising. Limitations of our study include short follow-up and the lack of a control group; however, we demonstrated superior outcomes with the Aberration-Free compared with standard ablation profiles.

CONCLUSION

In summary, this study demonstrated that aberration-neutral profile definitions, which are not standard in refractive surgery, yield good visual, optical, and refractive results. Preoperative refractions were reduced to subclinical values, with no clinically relevant induction of HOAs. As demonstrated here, aberration-neutral ablation profiles have the potential to replace currently used standard algorithms for noncustomized corrections. ■

Maria Clara Arbelaez, MD, practices at the Muscat Eye Laser Center, Muscat, Sultanate of Oman. Dr. Arbelaez states that she has no financial interest in the products or companies mentioned. She may be reached at tel: +96824691414; fax: +96824601212; e-mail: drmaria@omantel.net.om.

Samuel Arba Mosquera, MS, is with the Grupo de Investigación de Cirugía Refractiva y Calidad de Visión, Instituto de Oftalmobiología Aplicada, University of Valladolid, Valladolid, Spain, and Schwind eye-tech-solutions, Kleinostheim, Germany.

1. Munnerlyn CR, Koons SJ, Marshall J. Photorefractive keratectomy: a technique for laser refractive surgery. *J Cataract Refract Surg.* 1988;14:46-52.

2. Alio JL, Belda JI, Osman AA, Shalaby AM. Topography-guided laser in situ keratomileusis (TOPOLINK) to correct irregular astigmatism after previous refractive surgery. *J Refract Surg.* 2003;19:516-527.
3. Mrochen M, Kaemmerer M, Seiler T. Clinical results of wavefront-guided laser in situ keratomileusis 3 months after surgery. *J Cataract Refract Surg.* 2001;27:201-207.
4. Liang J, Grimm B, Goelz S, Bille JF. Objective measurement of wave aberrations of the human eye with the use of a Hartmann-Shack wave-front sensor. *J Opt Soc Am A Opt Image Sci Vis.* 1994;11:1949-1957.
5. Salmon TO. Corneal contribution to the Wavefront aberration of the eye. *PhD Dissertation.* 1999:70.
6. Mrochen M, Jankov M, Bueeler M, Seiler T. Correlation Between Corneal and Total Wavefront Aberrations in Myopic Eyes. *J Refract Surg.* 2003;19:104-112.
7. Moreno-Barriuso E, Lloves JM, Marcos S. Ocular Aberrations before and after myopic corneal refractive surgery: LASIK-induced changes measured with LASER ray tracing. *Invest Ophthalmol Vis Sci.* 2001; 42:1396-1403.
8. Mastropasqua L, Toto L, Zuppari E, Nubile M, Carpineto P, Di Nicola M, Ballone E. Photorefractive keratectomy with aspheric profile of ablation versus conventional photorefractive keratectomy for myopia correction: six-month controlled clinical trial. *J Cataract Refract Surg.* 2006;32:109-116.
9. Mrochen M, Donetzky C, Wüllner C, Löffler J. Wavefront-optimized ablation profiles: Theoretical background. *J Cataract Refract Surg.* 2004;30:775-785.
10. Koller T, Iseli HP, Hafezi F, Mrochen M, Seiler T. Q-factor customized ablation profile for the correction of myopic astigmatism. *J Cataract Refract Surg.* 2006;32:584-589.
11. Mastropasqua L, Nubile M, Ciancaglini M, Toto L, Ballone E. Prospective randomized comparison of wavefront-guided and conventional photorefractive keratectomy for myopia with the meditec MEL 70 laser. *J Refract Surg.* 2004;20:422-431.
12. Chung SH, Lee IS, Lee YG, et al. Comparison of higher-order aberrations after wavefront-guided laser in situ keratomileusis and laser-assisted subepithelial keratectomy. *J Cataract Refract Surg.* 2006;32:779-784.
13. Buzzonetti L, Iarossi G, Valente P, et al. Comparison of wavefront aberration changes in the anterior corneal surface after laser-assisted subepithelial keratectomy and laser in situ keratomileusis: preliminary study. *J Cataract Refract Surg.* 2004;30:1929-1933.
14. Wang Z, Chen J, Yang B. Posterior corneal surface topographic changes after LASIK are related to residual corneal bed thickness. *Ophthalmology.* 1999;106:406-409.
15. Binder PS. Analysis of ectasia after laser in situ keratomileusis: risk factors. *J Cataract Refract Surg.* 2007;33:1530-1538.
16. Wirbelauer C, Aurich H, Pham DT. Online optical coherence pachymetry to evaluate intraoperative ablation parameters in LASIK. *Graefes Arch Clin Exp Ophthalmol.* 2007;245:775-781.
17. Dupps WJ Jr, Roberts C. Effect of acute biomechanical changes on corneal curvature after photokeratectomy. *J Refract Surg.* 2001;17: 658-669.
18. Mrochen M, Bueeler M. Aspheric optics: physical fundamentals. *Ophthalmology.* 2008;105:224-233.
19. Arba Mosquera S, de Ortueta D. Geometrical analysis of the loss of ablation efficiency at non-normal incidence. *Opt Express.* 2008;16:3877-3895.
20. Barbero S. Refractive power of a multilayer rotationally symmetric model of the human cornea and tear film. *J Opt Soc Am A Opt Image Sci Vis.* 2006;23:1578-1585.
21. Levy Y, Segal O, Avni I, Zadok D. Ocular higher-order aberrations in eyes with supernormal vision. *Am J Ophthalmol.* 2005;139:225-228.
22. Alió J, Galal A, Montalbán R, Piñero D. Corneal wavefront-guided LASIK retreatments for correction of highly aberrated corneas following refractive surgery. *J Refract Surg.* 2007;23:760-773.
23. Seo KY, Lee JB, Kang JJ, Lee ES, Kim EK. Comparison of higher-order aberrations after LASEK with a 6.0 mm ablation zone and a 6.5 mm ablation zone with blend zone. *J Cataract Refract Surg.* 2004;30:653-657.
24. Arbelaez MC, Vidal C, Arba Mosquera S. Clinical Outcomes of Corneal Vertex versus Central Pupil References with Aberration-free Ablation Strategies and LASIK. *Invest Ophthalmol Vis Sci.* 2008; Jul 24. [Epub ahead of print].
25. Vroman DT, Sandoval HP, Fernández de Castro LE, Kasper TJ, Holzer MP, Solomon KD. Effect of hinge location on corneal sensation and dry eye after laser in situ keratomileusis for myopia. *J Cataract Refract Surg.* 2005;31:1881-1887.
26. Slade SG. Thin-flap laser-assisted in situ keratomileusis. *Curr Opin Ophthalmol.* 2008; 19:325-329.
27. Wirbelauer C, Pham DT. Continuous monitoring of corneal thickness changes during LASIK with online optical coherence pachymetry. *J Cataract Refract Surg.* 2004;30:2559-2568.
28. Yoon G, MacRae S, Williams DR, Cox IG. Causes of spherical aberration induced by laser refractive surgery. *J Cataract Refract Surg.* 2005;31:127-135.
29. Hersh PS, Fry K, Blaker JW. Spherical aberration after laser in situ keratomileusis and photorefractive keratectomy. Clinical results and theoretical models of etiology. *J Cataract Refract Surg.* 2003;29:2096-2104.
30. Bende T, Seiler T, Wollensak J. Corneal Thermal Gradients. *Graefes Archive Ophthalmology.* 1988;226:277-280.